Virus Genes (2007) 35:857–873
DOI 10.1007/s11262-007-0136-6

Genomic sequence analysis of a nucleopolyhedrovirus isolated from the diamondback moth, *Plutella xylostella*

Robert L. Harrison · Dwight E. Lynn

Received: 30 May 2007 / Accepted: 27 June 2007 / Published online: 2 August 2007
© Springer Science+Business Media, LLC 2007

Abstract The CL3 plaque isolate of *Plutella xylostella* multiple nucleopolyhedrovirus (PlxyMNPV-CL3) exhibits a high degree of genetic similarity with the *Autographa californica* MNPV (AcMNPV) but is significantly more virulent against the diamondback moth, *P. xylostella*, than AcMNPV. To identify genetic differences between PlxyMNPV-CL3 and AcMNPV that may account for the difference in virulence against *P. xylostella*, the genome sequence of the CL3 plaque isolate of PlxyMNPV was determined and compared to the genome sequence of AcMNPV isolate C6. The PlxyMNPV genome is 134,417 bp, 523 bp larger than the AcMNPV-C6 genome, and the nucleotide sequence is almost completely co-linear with that of AcMNPV-C6. Of the 153 open reading frames (ORFs) identified in PlxyMNPV, 151 had homologues in AcMNPV-C6, with a mean amino acid sequence identity of 98.5%. The PlxyMNPV genome possessed two features previously reported for other variants of AcMNPV: (1) an extra *baculovirus repeated orf* (*bro*) sequence located between the *plxy29/ac30* and *sod* ORFs, and (2) the deletion of the AcMNPV *pnk/pnl* polynucleotide kinase/ligase gene. In addition, an 817 bp insert of unknown origin located between the *fp25K* and *lef-9* genes was discovered. This insert contained two small ORFs and was detected in both tissue culture- and larvae-derived PlxyMNPV DNA by PCR. Finally, the PlxyMNPV-CL3 *ie-2* gene encodes a product with a low level (37.3%) of amino acid sequence identity with the AcMNPV-C6 *ie-2* product. PlxyMNPV-CL3 apparently acquired this variant *ie2* gene by recombination with an undescribed nucleopolyhedrovirus.

Keywords Baculovirus · Nucleopolyhedrovirus · *Plutella xylostella* · PlxyMNPV · *Autographa californica* · AcMNPV · *ie-2* · Few polyhedra mutants

The nucleotide sequence data reported in this paper have been submitted to the GenBank nucleotide sequence database and have been assigned the accession numbers DQ457003 (PlxyMNPV-CL3), DQ482644 (AcMNPV-C6 *ac17*), DQ482645 (AcMNPV-C6 *ac52*), DQ482646 (AcMNPV-C6 *ac58/ac59*), DQ482647 (AcMNPV-C6 *ac106/ac107*), DQ482648 (AcMNPV-C6 *ac112/ac113*), DQ482649 (AcMNPV-C6 *odv-e18*), DQ482650 (AcMNPV-C6 *ac145*), DQ482651 (AcMNPV-C6 *arif-1*), and DQ482652 (AcMNPV-C6 *pep*).

R. L. Harrison (✉) · D. E. Lynn
Insect Biocontrol Laboratory, USDA Agricultural Research Service, Plant Sciences Institute, Building 011A, Room 214, BARC-W, 10300 Baltimore Avenue, Beltsville, MD 20705, USA
e-mail: Robert.L.Harrison@ars.usda.gov

D. E. Lynn
e-mail: Dwight.Lynn@ars.usda.gov

Introduction

Members of family Baculoviridae are DNA viruses that infect arthropods, with most baculoviruses described from the insect order Lepidoptera [1, 2]. Baculoviruses are further classified as nucleopolyhedroviruses (NPVs) or granuloviruses (GVs) on the basis of viral occlusion morphology. Baculoviruses infect and kill many species of lepidopteran pests of agriculture and forestry, as well as some species of sawflies (Hymentoptera) and mosquitoes (Diptera). They are harmless to vertebrates and plants, and have little or no impact on beneficial arthropod populations [3, 4].

Despite these advantages, baculoviruses have not been adopted for pest control on a wide-scale basis in the US and some other industrialized countries where effective

chemical insecticides are readily available. One potential impediment to the use and commercialization of baculovirus-based biopesticides is their narrow host range. A narrow host range is attractive from an integrated pest management standpoint. However, the need to produce and apply multiple baculoviruses in order to effectively control multiple pests occurring in a cropping system may not be appealing from an economic standpoint [5]. A greater understanding of the molecular genetic determinants of baculovirus host range and virulence may enable researchers to further exploit the insecticidal potential of baculoviruses.

The diamondback moth, *Plutella xylostella*, is a cosmopolitan pest of cruciferous crops that has demonstrated the ability to acquire resistance to every insecticidal compound used intensively against it [6]. Although the *Autographa californica* multiple nucleopolyhedrovirus (AcMNPV) is infectious towards *P. xylostella*, it exhibits a relatively low level of virulence towards this species [7, 8]. A nucleopolyhedrovirus previously had been isolated from infected larvae of *P. xylostella* [9]. This virus, *Plutella xylostella* multiple nucleopolyhedrovirus isolate CL3 (or PlxyMNPV-CL3), is significantly more virulent against *P. xylostella* larvae than both wild-type AcMNPV [9] and an isolate of AcMNPV selected for enhanced activity against *P. xylostella* [10]. Restriction enzyme digest and Southern blot analysis indicate that PlxyMNPV-CL3 is genetically very similar to AcMNPV [9, 11].

The comparison of genomes of closely related baculoviruses with differing host range or virulence profiles can facilitate identification of genes involved in host range or virulence. Towards this goal, the genomic sequence of PlxyMNPV-CL3 was determined and compared to that of AcMNPV-C6.

Materials and methods

Virus and cells

The AcMNPV isolate C6 [12] and PlxyMNPV isolate CL3 [9] were propagated in the Spodoptera frugiperda Sf9 cell line [13] and titered by plaque assay. Sf9 cells were grown in TNM-FH medium (SAFC Biosciences) supplemented with 10% fetal bovine serum (Invitrogen), antibiotics (10 U penicillin, 0.1 mg streptomycin, and 0.25 μg amphotericin B/mL; Sigma), and 0.1% Pluronic F-68 (SAFC Biosciences).

Viral DNA isolation and cloning

Heliothis virescens IPLB-HvE6s cells [14], which support replication of PlxyMNPV at high levels, were infected with PlxyMNPV-CL3 at an approximate multiplicity of infection (MOI) of 0.5 plaque-forming units (PFU)/cell. Budded virus (BV) was harvested from the medium of the infected cultures at 5 days post-infection (p.i.) and pelleted through a 25% w/w sucrose pad by centrifugation at 103,900 × *g* for 75 min.

PlxyMNPV-CL3 DNA was extracted from the BV pellet by incubation with 10 mM Tris–HCl pH 8.0–10 mM EDTA pH 8.0–0.25% SDS-500 μg/ml protease K for 3 h at 37°C. Viral DNA was purified by phenol–chloroform extraction and ethanol precipitation. The identity of the viral DNA was confirmed by digestion of DNA with restriction enzymes, agarose gel electrophoresis, and comparison of the restriction fragment patterns with previously published restriction digests for this virus [9, 11].

After re-suspension, PlxyMNPV-CL3 DNA was sheared with a GeneMachines Hydroshear device (Genomic Solutions) following the manufacturer's instructions. Fragments ranging in size from 0.8 to 2 kb were gel-purified and cloned into pBluescript II KS+ and pCR-Blunt II-TOPO (Invitrogen) plasmid vectors. After transformation into competent *E. coli* JM109 or TOP10 cells, cloned products were plated on LB-agar plates spread with X-gal. White colonies from the transformation were picked into 25 μl 10 mM Tris-0.1 mM EDTA-0.5% Triton X-100 and lysed by incubation at 100°C for 5 min.

PxMNPV-CL3 DNA also was isolated from polyhedra stocks of the virus that had been maintained exclusively in larvae [10]. Polyhedra were dissolved as previously described [15], and occluded virus (OV) was pelleted and DNA extracted as described above for BV.

DNA sequencing and sequence analysis

Cloned PlxyMNPV-CL3 sequence fragments were amplified from colony lysates (2 μl/lysate) by polymerase chain reaction (PCR) with plasmid vector-specific primers M13F (5′-TTGTAAAACGACGGCCAGT-3′) and M13R (5′-GGAAACAGCTATGACCATG-3′). To eliminate excess primers and deoxynucletides, the resulting PCR products were precipitated by incubation with an equal volume of 20% PEG-2.5 M NaCl for 30 min at 37°C. PCR products were pelleted by centrifugation, and washed twice with 80% ethanol.

The PCR products were sequenced using nested plasmid vector-specific primers T7 (5′-GTAATACGACTCACTATAGGG-3′) and either T3 (5′-AATTAACCCTCACTAAAGGGA-3′) or SP6 (5′-GCTATTTAGGTGACACTATAG-3′). Reactions were set up using the Applied Biosytems BigDye Terminator Cycle Sequencing kit with AmpliTaq DNA polymerase, and electrophoresed on an Applied Biosystems 3100 DNA sequencer.

DNA sequence data was compiled and analyzed with the software of the Lasergene suite (DNASTAR, Inc.). Gaps and ambiguities in the genome sequence were resolved by amplifying the corresponding regions of the sequence from viral DNA by PCR (40 pg DNA/reaction) with custom-designed primers and sequencing the PCR products. Selected regions of the genome sequence also were amplified from viral DNA isolated from larval-derived polyhedra and sequenced.

Open reading frames (ORFs) >50 codons in length that did not overlap larger ORFs by more than 75 nt were selected for further characterization. Additional ORFs with homologues in other baculovirus genomes also were characterized. Predicted amino acid sequence identities were obtained from the results of protein database searches using the standard protein-protein BLAST algorithm (http://www.ncbi.nlm.nih.gov/BLAST/).

Predicted amino acid sequences of selected genes from group I NPVs [16–23] were aligned by ClustalW [24] using Gonnet matrices with a gap penalty of either 10 or 15 and a gap extension penalty of 0.2 or 0.3 for both pairwise and multiple alignments. Phylogenetic inferences with amino acid alignments were performed with MEGA version 3.1 [25] using minimum evolution (ME) and maximum parsimony (MP) methods. ME and MP trees were sought by using a close-neighbor-interchange heuristic search, starting with either one initial neighbor-joining tree ME or 10 initial trees generated by random addition of sequences MP. For ME trees, Dayhoff matrix distances were estimated with a gamma shape parameter of 2.25. In both cases, the reliability of the trees was tested with bootstrap re-sampling using 1,000 replicates. Pairwise nucleotide sequence alignments were carried out using the Martinez/Needleman-Wunsch method of MegAlign (DNAStar, Inc.) with a gap penalty of 1.10 and a gap length penalty of 0.33. Alignment of *ie-2* nucleotide sequences was carried out with the GAP (Needleman-Wunsch) program of the Accelrys GCG package (version 11.1) with a gap weight of 2.0 and a length weight of 11.0.

Quantitation of viral growth

Sf9 cells were seeded in six-well plates (1×10^6 cells/well) and infected with AcMNPV-C6 and PlxyMNPV-CL3 at a MOI of 1 plaque-forming unit (PFU)/cell. Medium was harvested at 24, 48, and 72 hr p. i. from three well/virus/time point. Polyhedra were purified from cells at 96 hr p. i. (3 wells/virus) following the procedure of O'Reilly et al. [15]. The titer of budded virus in infected cell medium was assessed by plaque assay [13], and polyhedra were counted with a hemocytometer.

Results

Features of the PlxyMNPV-CL3 nucleotide sequence

A complete sequence of the PlxyMNPV-CL3 genome with 8.6X coverage was obtained. To facilitate comparison of the PlxyMNPV-CL3 and AcMNPV-C6 sequences, the first nucleotide position for the PlxyMNPV-CL3 genome sequence was set to the nucleotide that aligned with the first nucleotide of the AcMNPV-C6 sequence. The PlxyMNPV-CL3 genome was 134,417 bp in length, 523 bp larger than the AcMNPV-C6 genome, with a G+C content of 40.7%, which is identical to that of AcMNPV. The overall nucleotide sequence identity between PlxyMNPV-CL3 and AcMNPV-C6 was approximately 98.6%. The PlxyMNPV-CL3 sequence was almost completely co-linear with the AcMNPV-C6 sequence (Fig. 1, Table 1). one hundred fifty-three ORFs that equal or exceed 50 codons in length, have minimal (<75 bp) overlap with larger ORFs, or share significant sequence identity with previously characterized ORFs from other baculovirus genomes were identified in the PlxyMNPV-CL3 genome (Table 1). Of these ORFs, 151 have homologues in the AcMNPV-C6 genome. (Fig. 1, Table 1).

The high degree of nucleotide and amino acid sequence identity and the conservation of ORF content strongly indicated that PlxyMNPV-CL3 is a variant of AcMNPV. To confirm this relationship, phylogenetic trees were inferred from the concatenated partial amino acid sequences of polyhedrin and late expression factors 8 and 9 (*lef-8*, and *lef-9*) for PlxyMNPV-CL3 and a selection of other group I NPVs [16–21]. By this analysis, PlxyMNPV-CL3 grouped within a clade containing several isolates of AcMNPV (data not shown). PlxyMNPV-CL3 originally was plaque-purified from a granulovirus (GV) sample isolated from infected *P. xylostella* larvae [9]. Assuming that this virus is not a laboratory contaminant of the *P. xylostella* granulovirus sample, it is not likely to be derived from the same stock, population, or geographic area as the original isolate of AcMNPV described by Vail et al. [26].

Homologous regions and promoter motifs

Homologous repeat regions (*hr*s) are repeated sequences found in most baculovirus genomes that function as enhancers of gene expression and origins of DNA replication [27]. The PlxyMNPV-CL3 genome contained nine *hr*s consisting of the same 30 bp imperfect palindrome repeats found in AcMNPV *hr*s. The PlxyMNPV *hr*s occupied the same positions on the genome with respect to surrounding ORFs as the AcMNPV *hr*s (Fig. 1) and were numbered in the same order as the AcMNPV *hr*s. The number and

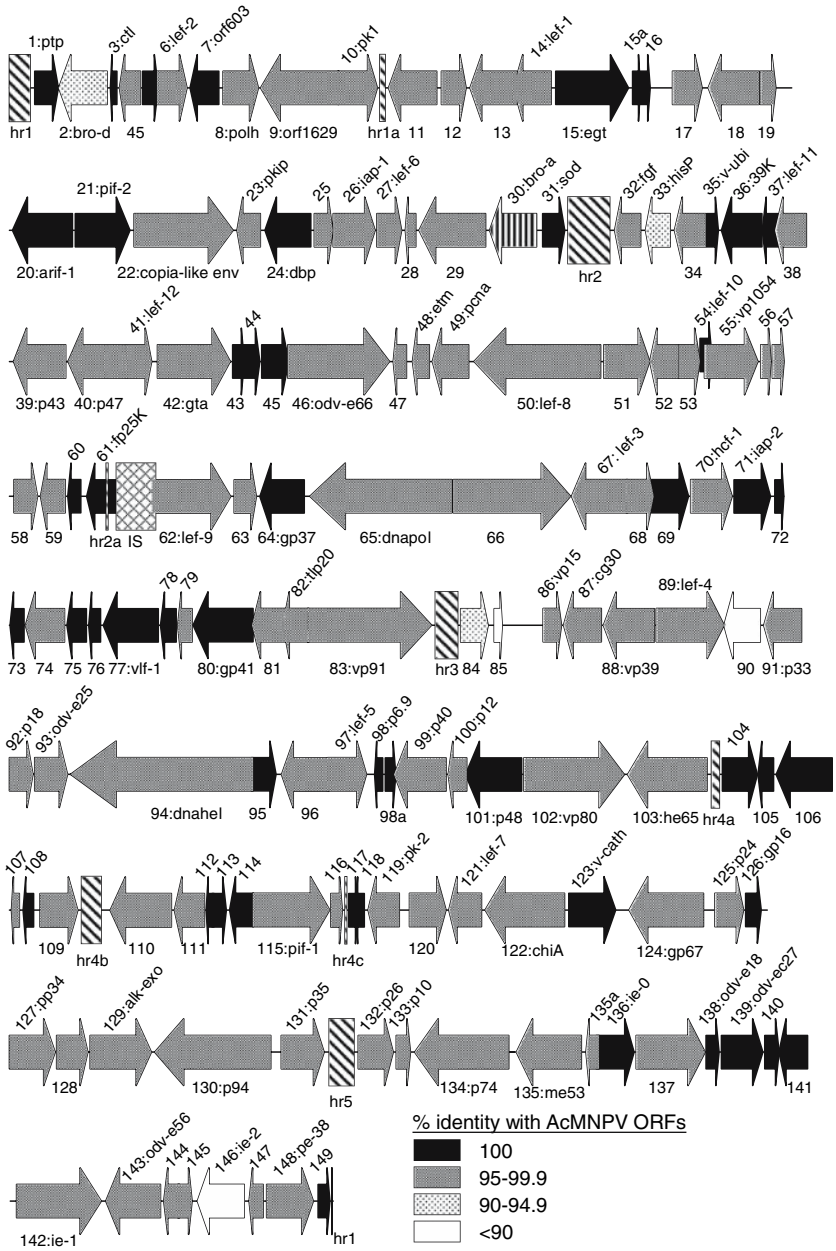

Fig. 1 Map of the ORFs and other features of the PlxyMNPV-CL3 genome. ORFs are represented by arrows, with the position and direction of the arrow indicating ORF position and orientation. The number of each ORF is displayed, with the name of the ORF following a colon. Homologous repeat regions (*hr*s) are represented by hatched boxes, and the 817 bp insertion sequence (IS) is represented by a cross-hatched box. The shading of the ORFs indicates the degree of predicted amino acid sequence similarity to AcMNPV homologues. The *bro-a* homologue (ORF 30), for which an AcMNPV homologue does not exist, is indicated by a vertically striped arrow

spacing of the palindrome repeats for some of the *hr*s differed between the two viruses (Table 1). A similar pattern of repeat sequence deletion and duplication has been observed upon comparison of the *hr*s of other closely related baculoviruses [21, 28–30].

A comparison of promoter motifs associated with PlxyMNPV-CL3 and AcMNPV-C6 homologous ORFs revealed differences in the presence of early and late promoter motifs for eight ORFs. PlxyMNPV ORFs *plxy36*, *plxy57*, *lef-9*, *hcf-1*, and *plxy85* contained initiator sites within 120 bp of the start codon that were preceded by TATA boxes (Table 1), while the AcMNPV homologues of these ORFs lacked these motifs. The early promoter motif CGTGC was present upstream of PlxyMNPV *ctl* and *plxy29*, but absent from the corresponding AcMNPV ORFs. Finally, *plxy29* and *plxy48* upstream regions contained the late promoter motif (A/T/G)TAAG, while the AcMNPV homologues for these ORFs did not.

ORF content and relatedness

Of the 151 ORFs that AcMNPV-C6 and PlxyMNPV-CL3 have in common, the average sequence identity for the predicted amino acid sequences is 98.5%, with 51 ORFs sharing 100% sequence identity and an additional 94 ORFs sharing >95% sequence identity (Fig. 1, Table 1). Of the

Table 1 ORFs and other features of PlxyMNPV-CL3

PlxyMNPV features					Comparison with other AcMNPV-like viruses					
					AcMNPV-C6		RoMNPV-R1		BmNPV-T3	
ORF/ feature	Name	Position[a]	aa (Da)[b]	Promoter motifs[c]	ORF (size)/*hr*	% ID (range)	ORF (size)/*hr*	% ID (range)	ORF (size)/*hr*	% ID (range)
	hr1 (5 repeats)	134406–134417; 1–441			*hr1* (5 repeats)		hr1 (4 repeats)		*hr1* (7 repeats)	
1	*ptp*	499 → 1005	168 (19288)	E, L	ac1 (168)	100 (168/168)	ro1 (168)	98.8 (166/168)	bm130 (168)	97 (163/168)
2	*bro-d*	1002 ← 2024	340 (39122)	L	ac2 (328)	94.6 (297/314)			bm131 (349)	82.8 (289/349)
3	*ctl*	2062 ← 2223	53 (5591)	E, L	ac3 (53)	100 (53/53)				
4		2273 ← 2728	151 (17605)	E	ac4 (151)	99.3 (150/151)	ro2 (151)	96.7 (146/151)	bm133 (151)	94.7 (143/151)
5		2757 → 3086	109 (12435	L	ac5 (109)	100 (109/109)	ro3 (109)	98.2 (107/109)	bm137 (109)	92.7 (101/109)
6	*lef-2*	3067 → 3699	210 (23869)	E, L	ac6 (210)	99.5 (209/210)	ro4 (210)	96.2 (202/210)	bm135 (210)	95.2 (200/210)
7	*orf603*	3737 ← 4342	201 (23612)	C	ac7 (201)	100 (201/201)	ro5 (211)	87.1 (183/210)		
8	*polh*	4498 → 5235	245 (28672)	L	ac8 (245)	99.6 (244/245)	ro6 (245)	90.2 (221/245)	bm1 (245)	85.7 (210/245)
9	*orf1629* (capsid)	5265 ← 6896	543 (60720)		ac9 (543)	99.4 (540/543)	ro7 (542)	92.7 (507/547)	bm2 (542)	90.7 (499/550)
10	*pk-1*	6895 → 7713	272 (31975)	L	ac10 (272)	97.4 (265/272)	ro8 (272)	98.9 (269/272)	bm3 (275)	97.4 (262/269)
	hr1a (2 repeats)	7725–7842			*hr1a* (2 repeats)		*hr1a* (1 repeat)			
11		7877 ← 8899	340 (40034)	C, E	ac11 (340)	99.4 (338/340)	ro9 (339)	95.0 (321/338)	bm4 (340)	93.2 (317/340)
12		9049 → 9585	178 (21075)	E	ac12 (217)	97.8 (175/179)	ro10 (192)	92.7 (166/179)		
13		9611 ← 10594	327 (38686)	L	ac13 (327)	99.7 (326/327)	ro11 (328)	95.7 (314/328)	bm5 (331)	92.7 (307/331)
14	*lef-1*	10486 ← 11286	266 (30711)		ac14 (266)	98.9 (263/266)	ro12 (267)	94.8 (253/267)	bm6 (270)	95.6 (258/270)
15	*egt*	11399 → 12919	506 (57033)	C	ac15 (506)	100 (506/506)	ro13 (506)	96.6 (489/506)	bm7 (506)	95.58 (483/506)
15a		12932 → 13099	55 (6072)		ac15a (55)	100 (55/55)	ro13a (55)	94.5 (52/55)	bm7a (53)	58.9 (33/56)
16	*bv/odv-e26*	13065 → 13289	74 (8343)		ac16 (225)	100 (74/74)	ro14 (225)	100 (74/74)	bm8 (229)	95.9 (71/74)
17		13711 → 14343	210 (23983)	C	ac17 (209)	99.0 (208/210)	ro15 (210)	95.7 (202/211)	bm9 (210)	95.7 (201/210)
18		14373 ← 15434	353 (40900)	E	ac18 (353)	99.2 (350/353)	ro16 (352)	97.2 (343/353)	bm10 (356)	93.0 (331/356)
19		15436 → 15762	108 (12185)	L	ac19 (108)	99.1 (107/108)	ro17 (108)	97.2 (105/108)	bm11 (110)	90.0 (99/110)
20	*arif-1*	16030 ← 17283	417 (47686)	C	ac20-ac21(417)	100 (417/417)	ro18 (413)	94.7 (395/417)	bm12 (440)	83.9 (366/436)
21	*pif-2*	17320 → 18468	382 (43778)	L	ac22 (382)	100 (382/382)	ro19 (382)	98.4 (376/382)	bm13 (382)	93.5 (357/382)
22	*copia-like env*	18532 → 20604	690 (79828)	L	ac23 (690)	99.6 (687/690)	ro20 (687)	95.1 (656/690)	bm14 (673)	88.7 (604/681)
23	*pkip*	20653 ← 21162	169 (19210)	L	ac24 (169)	98.2 (166/169)	ro21 (168)	97.6 (163/167)	bm15 (169)	92.9 (157/169)
24	*dbp*	21202 ← 22152	316 (36554)		ac25 (316)	100 (316/316)	ro22 (315)	98.7 (312/316)	bm16 (317)	95.9 (306/319)
25		22228 → 22617	129 (14671)	E, L	ac26 (129)	99.2 (128/129)	ro23 (129)	95.3 (123/129)	bm17 (129)	92.2 (119/129)
26	*iap-1*	22619 → 23479	286 (33290)	E	ac27 (286)	98.3 (281/286)	ro24 (286)	95.8 (274/286)	bm18 (292)	93.2 (272/292)
27	*lef-6*	23484 → 24005	173 (20421)	E	ac28 (173)	98.3 (170/173)	ro25 (174)	93.0 (160/172)	bm19 (173)	92.5 (160/173)
28		24065 ← 24280	71 (8541)		ac29 (71)	98.6 (70/71)	ro26 (71)	97.2 (69/71)	bm20 (71)	91.5 (65/71)

Table 1 continued

PlxyMNPV features					Comparison with other AcMNPV-like viruses					
					AcMNPV-C6		RoMNPV-R1		BmNPV-T3	
ORF/ feature	Name	Position[a]	aa (Da)[b]	Promoter motifs[c]	ORF (size)/*hr*	% ID (range)	ORF (size)/*hr*	% ID (range)	ORF (size)/*hr*	% ID (range)
29		24334 ← 25725	463 (54701	E, L	ac30 (463)	99.4 (460/463)	ro27 (463)	95.7 (443/463)	bm21 (472)	95.7 (443/463)
30	BmNPV *bro-a*	25794 ← 26762	322 (36114)						bm22 (317)	83.1 (270/325)
31	*sod*	26918 → 27373	151 (16182)	L	ac31 (151)	100 (151/151)	ro28 (151)	97.4 (147/151)	bm23 (151)	96.7 (146/151)
	hr2 (10 repeats)	27391–28255			*hr2* (8 repeats)		*hr2* (4 repeats)		*hr2L* (5 repeats)	
32	*fgf*	28335 ← 28880	181 (20659)	C	ac32 (181)	99.4 (180/181)	ro29 (181)	96.7 (175/181)	bm24 (182)	88.5 (161/182)
33	*hisP*	29027 ← 29551	174 (19863)	E, L	ac33 (182)	92.9 (169/182)	ro30 (181)	91.2 (165/181)		
34		29564 ← 30211	215 (24812)	L	ac34 (215)	98.6 (212/215)	ro31 (215)	98.1 (211/215)	bm25 (215)	96.3 (207/215)
35	*v-ubi*	30232 → 30465	77 (8653)	L	ac35 (77)	100 (77/77)	ro32 (77)	100 (77/77)	bm26 (77)	100 (77/77)
36	39*k*	30512 ← 31339	275 (31282)	C, L	ac36 (275)	100 (275/275)	ro33 (275)	93.1 (256/275)	bm27 (277)	92.1 (255/277)
37	*lef-11*	31333 ← 31671	112 (13129)	E	ac37 (112)	100 (112/112)	ro34 (112)	95.5 (107/112)	bm28 (112)	97.3 (109/112)
38		31634 ← 32284	216 (25239)	L	ac38 (216)	99.5 (215/216)	ro35 (216)	97.2 (210/216)	bm29 (217)	96.8 (210/217)
39	*p*43	32352 ← 33440	362 (43433)		ac39 (363)	99.2 (355/358)	ro36 (362)	93.4 (338/362)	bm30 (362)	92.0 (333/362)
40	*p*47	33448 ← 34653	401 (47510)	E	ac40 (401)	99 (397/401)	ro37 (401)	98.0 (393/401)	bm31 (399)	97.8 (392/401)
41	*lef-12*	34652 → 35197	181 (21069)	E	ac41 (181)	98.9 (179/181)	ro38 (181)	96.7 (175/181)	bm32 (183)	94.3 (164/174)
42	*gta*	35281 → 36801	506 (59151)		ac42 (506)	98.6 (499/506)	ro39 (505)	97.4 (493/506)	bm33 (506)	96.6 (489/506)
43		36815 → 37048	77 (8816)	L	ac43 (77)	100 (77/77)	ro40 (77)	96.1 (74/77)	bm34 (78)	91.0 (71/78)
44		37029 → 37424	131 (15603)	E	ac44 (131)	100 (131/131)	ro41 (131)	95.4 (125/131)	bm35 (131)	98.5 (129/131)
45		37426 → 38004	192 (22652)		ac45 (192)	100 (192/192)	ro42 (191)	92.7 (178/192)	bm36 (193)	89.1 (173/193)
46	*odv-e66*	37989 → 40103	704 (79031)	L	ac46 (704)	99.3 (699/704)	ro43 (701)	97.0 (683/704)	bm37 (702)	92.9 (658/708)
47		40209 ← 40475	88 (10466)	C	ac47 (88)	98.9 (87/88)	ro44 (89)	92.1 (82/89)	bm38 (89)	93.1 (81/87)
48	*etm*	40549 ← 40890	113 (12847)	E, L	ac48 (113)	97.3 (110/113)	ro45 (113)	92.9 (105/113)		
49	*pcna*	40914 ← 41684	256 (28639)		ac49 (285)	99.6 (255/256)	ro46 (<285)	95.7 (245/256)		
50	*lef-8*	41794 ← 44424	876 (101764)		ac50 (876)	99.8 (874/876)	ro47 (876)	97.7 (856/876)	bm39 (877)	97.3 (853/877)
51		44451 → 45407	318 (37582)		ac51 (318)	99.4 (316/318)	ro48 (318)	95.3 (303/318)	bm40 (319)	94.0 (300/319)
52		45398 ← 45982	194 (23232)	E	ac52 (194)	98.5 (191/194)	ro49 (194)	95.4 (185/194)	bm41 (194)	95.4 (185/194)
53		45984 → 46403	139 (17056)	L	ac53 (139)	99.3 (138/139)	ro50 (139)	98.6 (137/139)	bm42 (139)	96.4 (134/139)
54	*lef-10*	46400 → 46636	78 (8597)		ac53a (78)	100 (78/78)	ro51 (78)	96.2 (75/78)	bm42a (78)	96.2 (75/78)
55	*vp1054*	46494 → 47591	365 (42047)		ac54 (365)	99.5 (363/365)	ro52 (365)	98.4 (359/365)	bm43 (365)	95.6 (349/365)
56		47683 → 47904	73 (8164)		ac55 (73)	98.6 (72/73)	ro53 (73)	98.6 (72/73)	bm44 (77)	92.2 (71/77)
57		47906 → 48160	84 (9885)	C, L	ac56 (84)	98.8 (83/84)	ro54 (84)	98.8 (83/84)	bm45 (84)	92.8 (77/83)
58		48345 → 48830	161 (18995)	E	ac57 (161)	99.4 (160/161)	ro55 (161)	97.5 (157/161)	bm46 (161)	94.4 (152/161)

Table 1 continued

PlxyMNPV features					Comparison with other AcMNPV-like viruses					
					AcMNPV-C6		RoMNPV-R1		BmNPV-T3	
ORF/ feature	Name	Position[a]	aa (Da)[b]	Promoter motifs[c]	ORF (size)/*hr*	% ID (range)	ORF (size)/*hr*	% ID (range)	ORF (size)/*hr*	% ID (range)
59		48846 ← 49364	172 (20337)		ac58–ac59 (172)	99.4 (171/172	ro56 (172)	97.1 (167/172)	bm47 (171)	90.8 (158/174)
60		49376 ← 49639	87 (10148)	L	ac60 (87)	100 (87/87)	ro57 (87)	100 (87/87)	bm48 (83)	87.5 (77/88)
61	*fp25K*	49786 ← 50472	228 (26900)	L	ac61 (214)	100 (214/214)	ro58 (214)	99.1 (212/214)	bm49 (214)	96.7 (207/214)
	hr2a (1 repeat)	49952–49981			*hr2a* (1 repeat)		*hr2a* (1 repeat)			
	Insertion sequence	50439–51255								
62	*lef-9*	51208 → 52824	538 (62122)	C	ac62 (516)	99.2 (512/516)	ro59 (519)	99.2 (512/516)	bm50 (490)	99.2 (486/490)
63		52885 → 53352	155 (18447)	C	ac63 (155)	98.7 (153/155)	ro60 (156)	96.1 (148/154)	bm51 (155)	92.9 (144/155)
64	*gp37*	53370 ← 54281	303 (34926)	L	ac64 (302)	100 (302/302)	ro61 (302)	96.4 (291/302)	bm52 (294)	95.9 (281/293)
65	*dnapol*	54419 ← 57376	985 (114479)	E	ac65 (984)	99.6 (981/985)	ro62 (985)	97.0 (955/985)	bm53 (986)	96.2 (949/986)
66		57385 → 59811	808 (93911)	L	ac66 (808)	99.3 (802/808)	ro63 (810)	95.1 (771/811)	bm54 (805)	92.6 (752/812)
67	*lef-3*	59814 ← 60971	385 (44608)		ac67 (385)	99.5 (383/385)	ro64 (385)	97.7 (376/385)	bm55 (385)	92.2 (355/385)
68		60813 → 61391	192 (22362)		ac68 (192)	99.5 (191/192)	ro65 (192)	95.8 (184/192)	bm56 (134)	93.3 (123/134)
69		61369 → 62157	262 (30355)		ac69 (262)	100 (262/262)	ro66 (262)	96.6 (253/262)	bm57 (262)	97.7 (256/262)
70	*hcf-1*	62203 → 63075	290 (34356)	C	ac70 (290)	99.3 (288/290)	ro67 (290)	83.8 (243/290)		
71	*iap-2*	63109 → 63858	249 (28621)	L	ac71 (249)	100 (249/249)	ro68 (249)	94.8 (236/249)	bm58 (249)	95.6 (238/249)
72		63917 → 64099	60 (7068)	C,E,L	ac72 (60)	100 (60/60)	ro69 (60)	98.3 (59/60)	bm58a (60)	88.3 (53/60)
73		64108 ← 64407	99 (11526)	E, L	ac73 (99)	100 (99/99)	ro70 (99)	98.0 (97/99)	bm59 (99)	87.9 (87/99)
74		64404 ← 65201	265 (30556)	L	ac74 (265)	99.2 (263/265)	ro71 (262)	94.7 (251/265)	bm60 (268)	91 (244/268)
75		65219 ← 65620	133 (15512)	L	ac75 (133)	100 (133/133)	ro72 (133)	100 (133/133)	bm61 (133)	96.2 (128/133)
76		65636 ← 65890	84 (9440)	E,L	ac76 (84)	100 (84/84)	ro73 (84)	100 (84/84)	bm62 (85)	96.5 (82/85)
77	*vlf-1*	65906 ← 67045	379 (44364)	L	ac77 (379)	100 (379/379)	ro74 (380)	99.2 (377/380)	bm63 (379)	98.2 (372/379)
78		67052 ← 67381	109 (12545)	L	ac78 (109)	100 (109/109)	ro75 (109)	99.1 (108/109)	bm64 (110)	93.6 (103/110)
79		67384 ← 67698	104 (12213)		ac79 (104)	99 (103/104)	ro76 (104)	96.2 (100/104)	bm65 (104)	100 (104/104)
80	*gp41*	67701 ← 68930	409 (45382	L	ac80 (409)	100 (409/409)	ro77 (409)	99.0 (405/409)	bm66 (403)	94.4 (387/410)
81		68920 ← 69621	233 (26865)	E,L	ac81 (233)	99.6 (232/233)	ro78 (233)	97.4 (227/233)	bm67 (234)	92.7 (215/232)
82	*telokinin-like*	69470 ← 70012	180 (19811)	L	ac82 (180)	97,8 (176/180)	ro79 (180)	96.7 (174/180)	bm68 (181)	86.7 (157/181)
83	*vp91* (capsid)	69978 → 72539	853 (96964)	L	ac83 (847)	98.8 (843/853)	ro80 (856)	96.1 (820/853)	bm69 (839)	90.6 (773/853)
	hr3 (5 repeats)	72580–73046			*hr3* (8 repeats)		*hr3* (7 repeats)		*hr3* (6 repeats)	
84		73078 → 73641	187 (21581)		ac84 (188)	91.5 (172/188)	ro81 (164)	83.1 (133/160)		
85		73842 → 74003	53 (6281)	C	ac85 (53)	84.9 (45/53)	ro82 (53)	84.9 (45/53)		
86	*vp15* (capsid)	74895 → 75275	126 (15047)	C,E	ac87 (126)	98.4 (124/126)	ro84 (126)	98.4 (124/126)	bm70 (126)	96.0 (121/126)

Table 1 continued

PlxyMNPV features					Comparison with other AcMNPV-like viruses					
					AcMNPV-C6		RoMNPV-R1		BmNPV-T3	
ORF/ feature	Name	Position[a]	aa (Da)[b]	Promoter motifs[c]	ORF (size)/*hr*	% ID (range)	ORF (size)/*hr*	% ID (range)	ORF (size)/*hr*	% ID (range)
87	*cg30*	75276 ← 76070	264 (30189)		ac88 (264)	97.7 (258/264)	ro85 (264)	97.7 (258/264)	bm71 (267)	91.8 (245/267)
88	*vp39* (capsid)	76073 ← 77116	347 (38808)	L	ac89 (347)	98.0 (339/346)	ro86 (347)	97.7 (338/346)	bm72 (350)	94.0 (329/350)
89	*lef-4*	77135 → 78529	464 (53909)		ac90 (464)	99.8 (463/464)	ro87 (464)	97.0 (450/464)	bm73 (465)	96.8 (450/465)
90		78526 ← 79278	250 (26820)	L	ac91 (224)	75.9 (192/253)	ro88 (237)	79.2 (202/255)	bm74 (154)	50.4 (126/250)
91	*p*33	79316 ← 80095	259 (30941)		ac92 (259)	99.6 (258/259)	ro89 (259)	99.6 (258/259)	bm75 (259)	96.9 (251/259)
92	*p*18	80094 → 80579	161 (18352)		ac93 (161)	99.4 (160/161)	ro90 (161)	97.5 (157/161)	bm76 (161)	98.1 (158/161)
93	*odv-e25*	80588 → 81274	228 (25556)	E,L	ac94 (228)	99.6 (227/228)	ro91 (228)	97.4 (222/228)	bm77 (228)	90.8 (207/228)
94	*dnahel*	81311 ← 84976	1221 (143257)	E, L	ac95 (1221)	99.7 (1217/1221)	ro92 (1221)	98.4 (1201/1221)	bm78 (1222)	95.8 (1171/1222)
95		84963 → 85484	173 (19840)		ac96 (173)	100 (173/173)	ro93 (173)	97.7 (169/173)	bm79 (182)	94.7 (161/170)
96		85627 ← 86589	320 (38022)	E, L	ac98 (320)	99.7 (319/320)	ro94 (320)	98.4 (315/320)	bm82 (320)	93.1 (296/318)
97	*lef-5*	86524 → 87321	265 (30996)		ac99 (265)	99.6 (264/265)	ro95 (265)	97.7 (259/265)	bm83 (265)	96.6 (256/265)
98	*p*6.9	87485 ← 87318	55 (6885)	L	ac100 (55)	100 (55/55)	ro96 (55)	100 (55/55)	bm84 (65)	78.5 (51/65)
98a		87356 → 87580	74 (8396)		ac100a (74)	100 (74/74)	ro96a (74)	100 (74/74)		
99	*p*40	87527 ← 88612	361 (41567)	L	ac101 (361)	99.4 (359/361)	ro97 (361)	98.6 (356/361)	bm85 (362)	96.1 (348/362)
100	*p*12	88632 ← 89000	122 (13347)	E, L	ac102 (122)	99.2 (121/122)	ro98 (121)	94.3 (115/122)	bm86 (123)	91.1 (112/123)
101	*p*48	88981 ← 90144	387 (45313)	L	ac103 (387)	100 (387/387)	ro99 (387)	98.4 (381/387)	bm87 (387)	95.6 (370/387)
102	*vp80*	90170 → 92245	691 (79910)	L	ac104 (691)	99.7 (689/691)	ro100 (693)	97.0 (672/693)	bm88 (692)	96.4 (667/692)
103	*he65*	92273 ← 93934	553 (65594)	C, L	ac105 (553)	98.6 (545/553)	ro101 (572)	95.5 (526/551)	bm89 (289)	94.8 (273/288)
	hr4a (2 repeats)	94061–94210			*hr4a* (2 repeats)		*hr4a* (1 repeat)		*hr4L* (3 repeats)	
104		94280 → 95011	243 (28285)	L	ac106–ac107 (243)	100 (243/243)	ro102 (245)	98.0 (240/245)	bm90 (249)	93.6 (233/249)
105		95012 ← 95329	105 (11840)	L	ac108 (105)	100 (105/105)	ro103 (105)	97.1 (101/104)	bm91 (105)	96.2 (100/104)
106		95341 ← 96513	390 (44803)	E, L	ac109 (390)	100 (390/390)	ro104 (390)	99.0 (386/390)	bm92 (391)	96.2 (376/391)
107		96549 ← 96719	56 (6814)	L	ac110 (56)	98.2 (55/56)	ro105 (56)	96.4 (54/56)		
108		96768 ← 96971	67 (8169)	E	ac111 (67)	100 (67/67)	ro106 (67)	88.1 (59/67)	bm93 (67)	88.1 (59/67)
109		97141 → 97917	258 (30992)	C	ac112–ac113 (258)	99.2 (256/258)	ro107 (254)	93.4 (241/258)		
	hr4b (4 repeats)	98016–98409			*hr4b* (5 repeats)		*hr4b* (4 repeats)		*hr4R* (2 repeats)	
110		98414 ← 99688	424 (49249)	E, L	ac114 (424)	99.1 (420/424)	ro108 (425)	97.2 (413/425)	bm94 (424)	95.5 (405/424)
111		99710 ← 100324	204 (23007)	E, L	ac115 (204)	99 (202/204)	ro109 (204)	97.1 (198/204)	bm95 (204)	92.2 (188/204)
112		100332 ← 100502	56 (6426)		ac116 (56)	100 (56/56)	ro110 (56)	87.5 (49/56)	bm95a (56)	85.7 (48/56)

Table 1 continued

PlxyMNPV features					Comparison with other AcMNPV-like viruses					
					AcMNPV-C6		RoMNPV-R1		BmNPV-T3	
ORF/ feature	Name	Position[a]	aa (Da)[b]	Promoter motifs[c]	ORF (size)/*hr*	% ID (range)	ORF (size)/*hr*	% ID (range)	ORF (size)/*hr*	% ID (range)
113		100438 → 100725	95 (10992)	C	ac117 (95)	100 (95/95)	ro111 (93)	95.7 (88/92)	bm96 (95)	94.7 (90/95)
114		100759 ← 101232	157 (18710)		ac118 (157)	100 (157/157)	ro112 (157)	93.6 (147/157)		
115	*pif-1*	101227 → 102819	530 (59793)	L	ac119 (530)	99.2 (526/530)	ro113 (530)	97.5 (517/530)	bm97 (527)	84.7 (450/531)
116		102824 → 103072	82 (9533)	L	ac120 (82)	98.8 (81/82)	ro114 (82)	93.9 (77/82)	bm98 (82)	95.1 (78/82)
	hr4c (1 repeat)	103134–103163			*hr4c* (1 repeat)		*hr4c* (1 repeat)			
117		103175 → 103351	58 (6705)		ac121 (58)	100 (58/58)				
118		103241 ← 103429	62 (7216)		ac122 (62)	100 (62/62)	ro115 (62)	98.4 (61/62)	bm99 (61)	90.3 (56/62)
119	*gcn2/pk-2*	103492 ← 104139	215 (24963)	E, L	ac123 (215)	98.6 (212/215)	ro116 (215)	91.6 (197/215)	bm100 (225)	95.3 (204/214)
120		104321 → 105064	247 (28524)	E, L	ac124 (247)	98 (242/247)	ro117 (247)	94.3 (233/247)	bm101 (244)	86.6 (214/247)
121	*lef-7*	105081 ← 105761	226 (26513)		ac125 (226)	96.9 (219/226)	ro118 (226)	92.9 (210/226)	bm102 (227)	87.2 (197/226)
122	*chiA*	105810 ← 107465	551 (61527)	L	ac126 (551)	99.1 (546/551)	ro119 (551)	97.1 (535/551)	bm103 (552)	95.7 (528/552)
123	*v-cath*	107513 → 108484	323 (36938)	E, L	ac127 (323)	100 (323/323)	ro120 (323)	99.1 (320/323)	bm104 (323)	96.3 (311/323)
124	*gp67*	108708 ← 110246	512 (58539)	E, C, L	ac128 (512)	99.8 (511/512)	ro121 (529)	98.4 (504/512)	bm105 (530)	95.5 (490/513)
125	*p*24 (capsid)	110429 → 111025	198 (22096)	L	ac129 (198)	99.5 (197/198)	ro122 (198)	93.4 (185/198)	bm106 (195)	92.4 (183/198)
126	*gp16*	111053 → 111373	106 (12112)	L	ac130 (106)	100 (106/106)	ro123 (106)	99.1 (105/106)	bm107 (106)	100 (106/106)
127	*pp34*	111432 → 112370	312 (35439)	E	ac131 (322)	96.2 (310/322)	ro124 (321)	96.0 (308/321)	bm108 (315)	91.2 (291/319)
128		112373 → 113032	219 (25156)	L	ac132 (219)	98.2 (215/219)	ro125 (223)	88.8 (198/223)	bm109 (220)	93.6 (206/220)
129	*alk-exo*	113060 → 114322	420 (48349)	L	ac133 (419)	99.0 (416/420)	ro126 (420)	97.4 (409/420)	bm110 (420)	95.5 (401/420)
130	*p*94	114373 ← 116784	803 (94572)		ac134 (803)	99.1 (796/803)	ro127 (803)	94.9 (759/800)	bm110a (57)	92.0 (46/50)
131	*p*35	116995 → 117894	299 (34828)	C, L	ac135 (299)	99.7 (298/299)	ro128 (300)	93.7 (281/300)	bm112 (299)	90.3 (270/299)
	hr5 (6 repeats)	117943–118456			*hr5* (6 repeats)		*hr5* (5 repeats)		*hr5* (8 repeats)	
132	*p*26	118552 → 119274	240 (27269)		ac136 (240)	99.2 (238/240)	ro129 (240)	96.3 (231/240)	bm113 (240)	93.8 (225/240)
133	*p*10	119348 → 119632	94 (10296)	L	ac137 (94)	98.9 (93/94)	ro130 (94)	95.7 (90/94)	bm114 (70)	88.6 (62/70)
134	*p*74	119644 ← 121581	645 (73999)	L	ac138 (645)	99.2 (640/645)	ro131 (645)	98.3 (639/645)	bm115 (645)	91.5 (590/645)
135	*me53*	121747 ← 123096	449 (52644)	C, E, L	ac139 (449)	98.4 (442/449)	ro132 (450)	95.6 (431/451)	bm116 (451)	91.2 (414/454)
135a		123180 ← 123446	88 (9803)		ac139a (67)	98.5 (66/67)	ro132a (67)	93.8 (60/64)		
136	*ie-0*	123374 → 124159	261 (30109)	C, L	ac141 (261)	100 (261/261)	ro133 (261)	98.5 (257/261)	bm117 (261)	96.9 (253/261)
137		124174 → 125607	477 (55431)	E, L	ac142 (477)	99.8 (476/477)	ro134 (478)	99.6 (473/475)	bm118 (476)	98.7 (470/476)
138	*odv-e18*	125609 → 125881	90 (9558)	L	ac143 (90)	100 (90/90)	ro135 (90)	90 (81/90)	bm119 (101)	76.2 (77/101)
139	*odv-ec27*	125897 → 126769	290 (33528)	L	ac144 (290)	100 (290/290)	ro136 (290)	100 (290/290)	bm120 (290)	99 (287/290)
140		126784 → 127071	95 (11038)	L	ac145 (95)	100 (95/95)	ro137 (95)	96.8 (92/95)	bm121 (95)	93.7 (89/95)
141		127066 ← 127671	201 (22881)		ac146 (201)	100 (201/201)	ro138 (201)	98.0 (197/201)	bm122 (201)	96.5 (194/201)

Table 1 continued

PlxyMNPV features					Comparison with other AcMNPV-like viruses					
					AcMNPV-C6		RoMNPV-R1		BmNPV-T3	
ORF/feature	Name	Position[a]	aa (Da)[b]	Promoter motifs[c]	ORF (size)/*hr*	% ID (range)	ORF (size)/*hr*	% ID (range)	ORF (size)/*hr*	% ID (range)
142	*ie-1*	127737 → 129485	582 (66880)	C	ac147 (582)	99.8 (581/582)	ro139 (580)	96.9 (565/583)	bm123 (584)	95.4 (557/584)
143	*odv-e56*	129547 ← 130680	377 (40898)	L	ac148 (376)	99.2 (374/377)	ro140 (378)	96.3 (364/378)	bm124 (375)	83.0 (313/377)
144		130709 ← 131032	107 (12341)		ac149 (107)	96.3 (103/107)	ro141 (107)	96.3 (103/107)	bm125 (106)	87.5 (91/104)
145		131013 → 131300	95 (11018)		ac150 (99)	97.8 (91/93)	ro142 (97)	82.8 (77/93)	bm126 (115)	65.4 (68/104)
146	*ie-2*	131397 ← 132563	388 (43672)	C,E,L	ac151 (408)	37.3 (154/413)	ro143 (407)	38.0 (156/410)	bm127 (422)	37.6 (159/423)
147		132625 ← 132909	94 (11018)		ac152 (92)	98.4 (60/61)	ro144 (92)	85.2 (52/61)		
148	*pe38*	133048 → 134013	321 (37518)	C,E,L	ac153 (321)	98.4 (316/321)	ro145 (323)	89.2 (290/325)	bm128 (309)	85.5 (277/324)
149		134114 → 134359	81 (9421)	C,L	ac154 (81)	100 (81/81)	ro146 (80)	92.6 (75/81)	bm129 (77)	82.9 (68/82)

[a] Direction of ORF in the PlxyMNPV genome is indicated by the arrow

[b] Number of amino acids encoded by ORF and mass in daltons

[c] Promoter motifs present upstream of ORF. C, Cap site (initiator) CA(G/T)T 120 bp upstream of start codon, preceded by a TATA box TATA(A/T)A(A/T) within 40 bp; E, early promoter motif CGTGC, 210 bp upstream of start codon; L, Late promoter motif (A/T/G)TAAG 120 bp upstream of start codon

remaining six ORFs, *plxy2*(*bro-d*), *plxy33* (*hisP*), *plxy84*, *plxy85*, and *plxy90* have amino sequence identities of 94.6%, 92.9%, 91.5%, 84.9%, and 75.9% with their corresponding AcMNPV-C6 homologues. The *plxy85* ORF and homologues in AcMNPV-C6 and RoMNPV-R1 shared significant amino acid sequence identity (50% over a 34-amino acid range) with a *Hyposoter didymator* ichovirus ORF encoding a 11.8 kDa product of unknown function [31] and a similar ORF from *Hyposoter fugitivus*ichnovirus (data not shown). Alignment of *plxy85* and *plxy90* homologues from AcMNPV-C6, PlxyMNPV-CL3, and RoMNPV-R1 revealed a significantly stronger degree of sequence conservation between the AcMNPV and RoMNPV ORFs than between the AcMNPV and PlxyMNPV ORFs, even though the average amino acid sequence identity between AcMNPV and RoMNPV homologous ORFs overall (95.4 ± 6.02%) is lower than that between AcMNPV and PlxyMNPV ORFs (98.5 ± 5.6%).

The PlxyMNPV-CL3 genome had two features previously reported for other AcMNPV variants [32]: (1) an extra baculovirus repeated ORF (*bro*) that is a homologue of *Bombyx mori* NPV (BmNPV) *bro-a*, and (2) the deletion of a large portion of *ac86* (*pnk/pnl*; Table 1). The additional *bro* sequence in PlxyMNPV-CL3 occurred between *sod* and *ac30/plxy29*, next to *hr2*, and in the same position where *bro-a* is found in BmNPV (Table 1). This *bro* sequence shared 83.1% amino acid sequence identity with BmNPV *bro-a* and 99.7% amino acid sequence identity with a *bro* found in the corresponding location of an AcMNPV variant isolated from *Spodoptera litura* larvae [32]. Homologues of the *bro* ORF are present in multiple copies in the genomes of baculoviruses and other insect viruses, as well as bacteriophages and bacterial transposons [33]. The BRO proteins of BmNPV are associated with nucleoprotein complexes, bind nucleic acids [34], and may be required for viral replication in some circumstances [33, 35]. AcMNPV only has one *bro*, while RoMNPV has none [21].

The *ac86* ORF deletion occurred in a region adjacent to *hr3* that is highly variable among group I NPVs [22]. The *ac86* ORF encodes a product with sequence similarity to two separate phage T4 enzymes, an ATP-dependent RNA ligase and a polynucleotide 5′-kinase/3′-phosphatase. The protein encoded by *ac86* has been shown to have adenylyltransferase, RNA ligase, polynucleotide kinase, and polynucleotide phosphatase activities [36]. However, *pnk/pnl* is dispensable for viral replication [37]. A naturally occurring variant of AcMNPV, isolate 1.2, also bears a deletion within *ac86* [37]. Comparison of the *ac86* region of AcMNPV-1.2 with PlxyMNPV-CL3 revealed that the deletion endpoints are conserved in these two viruses. The overall nucleotide sequence identity in this region was also

higher between AcMNPV-1.2 and PlxyMNPV-CL3 (98%) than between AcMNPV-C6 and PlxyMNPV-CL3 (93.1%). In contrast, RoMNPV-R1 has an intact *ac86* ORF and shares 99.8% nucleotide sequence identity with AcMNPV-C6 in this region.

A number of PlxyMNPV ORFs exhibited a high degree of sequence similarity with their AcMNPV homologues, but differed significantly in terms of ORF length or structure. As reported for RoMNPV-R1 [21], the PlxyMNPV-CL3 homologues of four pairs of adjacent AcMNPV ORFs (*ac20*/*ac21*, *ac58*/*ac59*, *ac106*/*ac107*, and *ac112*/*ac113*) were fused together into single ORFs (*plxy20*, *plxy59*, *plxy104*, and *plxy109*, respectively). Re-sequencing of these regions in AcMNPV-C6 previously had found that these ORFs are also fused in the stock of AcMNPV-C6 used in this study [21]. Five PlxyMNPV ORFs (*plxy17*, *plxy52*, *pp34*, *odv-e18*, and *plxy141*) were longer than the homologous AcMNPV ORFs and matched the ORF lengths reported for RoMNPV-R1 homologues [21]. These ORFs previously had been amplified and re-sequenced from AcMNPV-C6 [21] and found to differ from the lengths reported by Ayres et al. (1994) [17] and match the sizes of the corresponding RoMNPV-R1 homologues. The *plxy12*, *plxy16*, and *plxy135a* ORFs contained substitutions and deletions that significantly lengthened or shortened the ORFs compared to their homologues in AcMNPV (Table 1). The *plxy135a* ORF almost completely overlapped a separate 61-codon ORF (nt 123167 → 123349) that is identical to *ac140*. In the PlxyMNPV sequence corresponding to *ac97*, an 11-nt deletion led to a truncation of the ORF to 45 codons. As a consequence, an *ac97* homologue for PlxyMNPV was not listed in Table 1. The *plxy16* ORF was truncated by 150 codons relative to its AcMNPV homologue, *ac16*, due to a C to T mutation that changed a glutamine codon (CAG) to a stop codon (TAG). There are two small ORFs of 77 and 68 codons, ranging from nt 13086 ← 13316 and nt 13421 ← 13624 of the PlxyMNPV sequence, that would have been contained within an untruncated *ac16* homologous ORF. The predicted amino acid sequences of these ORFs did not match any other baculovirus ORFs or exhibit similarity to other sequences. The AcMNPV homologue of *plxy16* encodes BV/ODV-E26, a virion envelope protein that has been detected in complexes containing the FP25K protein and either cellular actin [38] or the ODV-E66 inner nuclear membrane targeting signal [39–41]. Insertional inactivation of AcMNPV*bv/odv-e26* has no detectable effect on infection and replication in cell lines and larvae of *S. frugiperda* or *Trichoplusia ni* [42]. Sequencing of the *plxy16* ORF amplified from larval stocks of virus confirmed that *plxy16* also was truncated in PlyxMNPV-CL3 that had been maintained in larvae.

PlxyMNPV-CL3 contains a variant form of *ie-2*

The nucleopolyhedrovirus *ie-2* gene is expressed early during infection and encodes a transcriptional regulator involved in stimulating transcription from baculovirus early gene promoters [43–45]. IE-2 also augments viral *hr*-mediated DNA replication and late promoter activation in transient assays [46, 47] and causes cell-cycle arrest in cultured lepidopteran cells [48]. The IE-2 proteins of AcMNPV and BmNPV localize to foci in the nucleus of transfected and virus-infected cells. At various times post-infection, IE-2 can be found at centers of viral DNA replication and also at a distinct class of nuclear domain known as promyelocytic leukaemia (PML) protein bodies that are adjacent to replication sites [49, 50].

In sharp contrast with other PlxyMNPV genes, the PlxyMNPV-CL3 *ie-2* amino acid sequence only shared 37% identity with the AcMNPV *ie-2* sequence. Even though the degree of amino acid sequence conservation was low, the closest matches to PlxyMNPV-CL3 IE-2 in a BLAST search were with the AcMNPV and RoMNPV IE-2 sequences. Serine-rich and proline/glutamine-rich domains involved in activation of a subset of baculovirus early promoters by AcMNPV IE-2 [51] were poorly conserved in the PlyxMNPV-CL3 sequence (Fig. 2A). A glutamate-rich region ranging from residues 167 to 180 aligned with an acidic domain required for transactivation. A RING finger domain required for cell cycle arrest, E3 ubiquitin ligase activity, and nuclear focus association [48, 50, 52] was strongly conserved in the PlxyMNPV-CL3 IE-2 sequence and among NPV IE-2 sequences in general. There was also significant sequence conservation within a predicted coiled-coil region (coiled-coil-II) involved in self-interaction and association with nuclear foci [50, 53]. Phylogenetic inference of IE-2 amino acid sequence relationships placed the PlxyMNPV-CL3 sequence within clade Ia of the group I NPVs, but the branch lengths indicated that PlxyMNPV-CL3 IE-2 was only distantly related to the IE-2 sequences of AcMNPV, RoMNPV, and BmNPV (Fig. 2B).

Alignment of the PlxyMNPV-CL3 and AcMNPV-C6 *ie-2* regions revealed a low degree of nucleotide sequence identity in an area encompassing the *ie-2* ORF, with many gaps inserted to achieve an optimal alignment (Fig. 3). A CAGT initiator (cap) site and a TATA box present upstream of the AcMNPV *ie-2* ORF were conserved in the PlxyMNPV-CL3 gene. The PlyxMNPV-CL3 nucleotide sequences flanking the *ie-2* gene showed the high degree of identity with the AcMNPV sequence present in the rest of the genome. This variant form of *ie-2* also was present in PlxyMNPV-CL3 DNA isolated from stocks maintained in larvae.

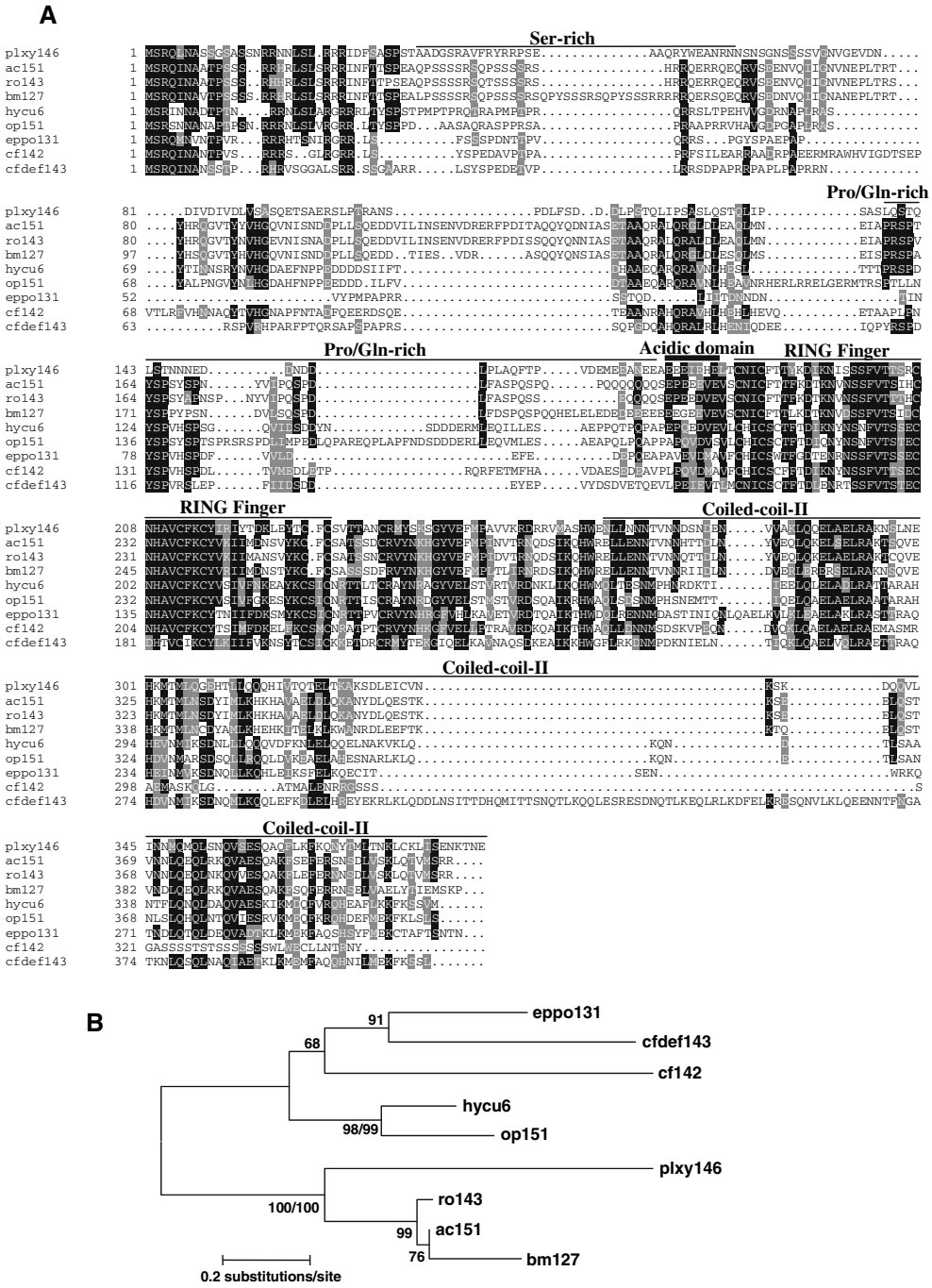

Fig. 2 **(A)** CLUSTAL-W alignment of IE-2 amino acid sequences. Identical residues occupying >50% of aligned positions are shaded in black, and residues similar to conserved residues or to each other are shaded in gray. Lines above the aligned sequences indicate the locations of different functional motifs. The acidic domain required for transcriptional activation is indicated with a thick line. **(B)** Phylogenetic analysis of IE-2 amino acid sequences. The figure contains a consensus ME phylogram inferred from the alignment in Fig. 2A with bootstrap values >50% shown at interior branches for ME and MP analysis (ME/MP) where they occur. The IE-2 sequences used derive from AcMNPV-C6 (*ac151*), *Bombyx mori* (Bm) NPV-T3 (*bm127*), *Rachiplusia ou* (Ro) MNPV-R1 (*ro143*), *Orgyia pseudotsugata* (Op) MNPV (*op151*), *Epiphyas postvittana* (Eppo) MNPV (*eppo131*), *Hyphantria cunea* (Hycu) NPV (*hycu6*; accession no. YP_473194), *Choristoneura fumiferana* (Cf) MNPV (*cf142*) [22], and *Choristoneura fumiferana* defective (CfDEF) NPV (*cfdef143*) [23]

PlxyMNPV-CL3 carries an insert between *fp25k* and *lef-9*

Examination of the aligned PlxyMNPV-CL3 and AcMNPV-C6 genomes revealed the presence of an 817 bp sequence lying between the *fp25k* and *lef-9* genes in PlxyMNPV-CL3 (Fig. 4). This sequence is not present in the AcMNPV-C6 genome. The 817 bp insert does not contain terminal inverted or direct repeats and is not flanked by a repeated viral "target" sequence, as has been reported previously for host transposable element inserts in baculovirus genomes [54–58]. A BLAST search with the insertion sequence turned up no significant matches on combined databases. The insert contains two small ORFs (<50 codons) extending from nt 50505 → 50687 and nt 50971 ← 51126 in the PlxyMNPV sequence. BLAST queries with these ORFs failed to detect significant sequence similarity with other sequences.

The 817 bp sequence was located between the *fp25k* ORF and the two TAAG sequences to which initiation of *fp25k*

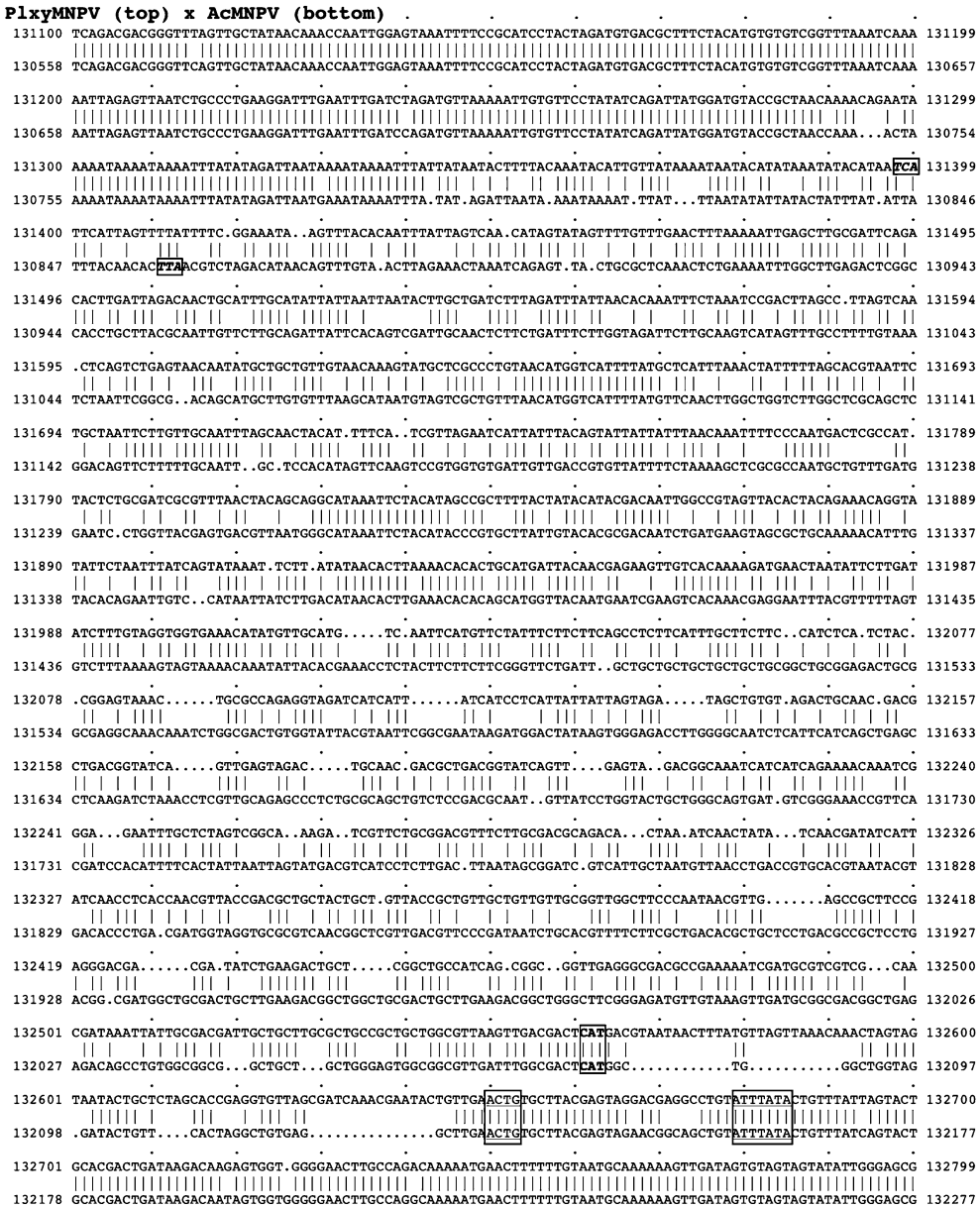

Fig. 3 Needleman and Wunsch (GAP) alignment of the *ie-2* regions of PlxyMNPV-CL3 (nt 131100 – 132799) and AcMNPV-C6 (130558 – 132277). The orientation of the *ie-2* ORFs is from right to left. The locations of TATA boxes and initiator sites (underlined), initiation codons (bold), and stop codons (bold italics) are indicated by boxes

transcription has been mapped in AcMNPV-E2 [59]. ATG codons occurred in the insert sequence upstream of, and in-frame with, the *fp25k* and *lef-9* ORFs (Fig. 4). As a result, these ORFs had an additional 14 and 22 N-terminal codons, respectively (Table 1). Three (A/T)TAAG late promoter motifs were located within the insertion sequence (IS) upstream of the extended *fp25k* ORF. Two CA(G/T)T initiator site and TATA box combinations were located in the insertion sequence upstream of the *lef-9* ORF.

Mutations in the *fp25k* gene cause a mutant phenotype, known as the few polyhedra (FP) phenotype. FP mutants bearing *fp25k*mutations produce fewer polyhedra and more BV than wild-type virus in tissue culture, and the viral occlusions produced by FP mutants contain few or no virions [56, 59–64]. Although the 817 bp insertion did not disrupt the PlxyMNPV-CL3 *fp25k* ORF, its presence in the promoter region of this gene may reduce or eliminate *fp25k* expression.

To determine if PlxyMNPV-CL3 exhibits any of the characteristics of the FP phenotype, Sf9 cells were infected with PlxyMNPV-CL3 and AcMNPV-C6 and BV and polyhedra production by the two viruses were quantified. PlxyMNPV-CL3 produced significantly more BV than AcMNPV-C6 at every time point measured, with the difference ranging from 2.6- to 4.3-fold (Fig. 5A). This result is consistent with the level of increase in BV production observed with AcMNPV FP mutants [60]. AcMNPV-C6 also produced approximately 2.1-fold more polyhedra than PlxyMNPV-CL3 in Sf9 cells (Fig. 5B).

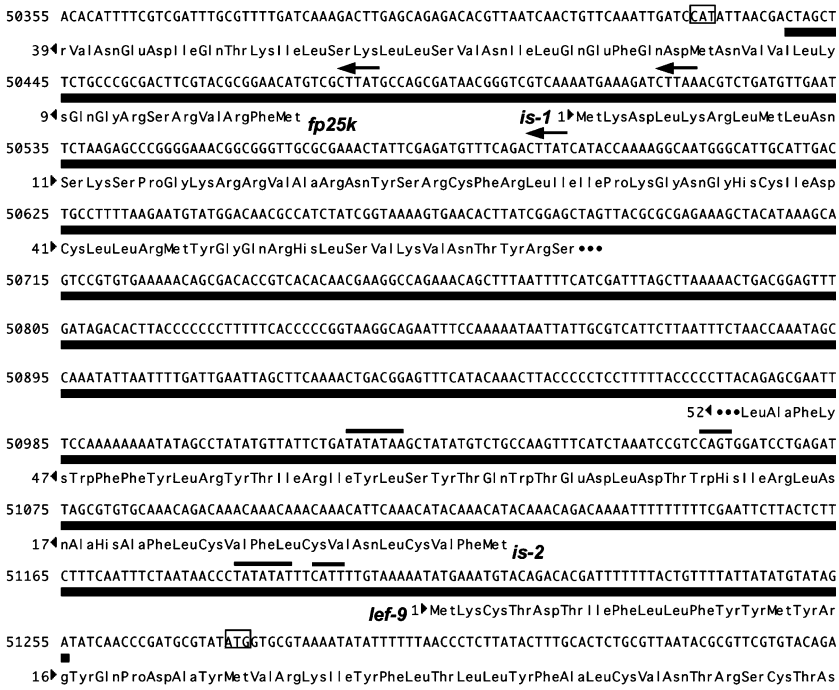

Fig. 4 Nucleotide sequence of an insertion in the promoter region of PlxyMNPV-CL3 *fp25k*. The insertion is denoted by a red bar underneath its sequence. Amino acid sequences for two small ORFs in the insertion (*is-1* and *is-2*) are shown underneath the ORFs. In addition, translation of the N-terminal portions of *lef-9* and *fp25k* are indicated, beginning at the in-frame ATGs present in the IS. The native initiation codons for these genes are indicated by boxes. Late promoter motifs (A/TTAAG) in the IS from which *fp25k* transcription potentially could initiate are indicated by arrows over the motifs. Paired TATA boxes and initiator sites (CAG/TT) in the insertion sequence that potentially could direct transcription of *lef-9* are indicated by black lines over the motifs

FP occlusions possess either no infectivity or drastically reduced infectivity towards larvae in bioassays [65–69]. Although FP mutants enjoy a selective advantage in cell culture due to their enhanced BV production, they are expected to be absent or maintained at low levels in virus isolates passaged by oral infection of larvae due to their impaired *per os* infectivity. However, Bull and co-workers [70] found that an AcMNPV FP mutant could maintain itself as a stable proportion of an NPV population after serial *per os* passages of an initial 1:1 mixture of wild-type: FP mutant virus through *T. ni* larvae. To determine if genotypes carrying the 817 bp insert were also present in preparations of PlxyMNPV-CL3 maintained in larvae, PCR amplification of the insert was carried out with PlxyMNPV-CL3 DNA purified from BV produced in IPLB-HvE6s cells and from two polyhedra stocks prepared from either *Spodoptera exigua* or *P. xylostella* larvae. The polyhedra stocks used in this experiment had been maintained exclusively by alternate passages in *S. exigua* and *P. xylostella* larvae [10]. Primers were designed which anneal to regions flanking the IS (PX77, PX79) and within the IS itself in either orientation (PX78, IS3; Fig. 6). Control reactions were carried out with primers (PX70 + PX71) that amplify a region encompassing parts of the *dnahel* and *plxy95* ORFs.

PCRs produced amplimers of the expected size for all templates. PCRs with primers but no template and template but no primers did not yield a product (Fig. 6). Amplimers for all templates were gel-purified and sequenced. The PX77 + PX78 and PX79 + IS3 amplimers from all three templates corresponded to the expected region of *fp25k* or *lef-9* and the IS, confirming the presence of the insertion sequence in larvae-derived stocks of PlxyMNPV-CL3. PCRs with primers flanking the IS also produced smaller, secondary amplimers of a size consistent with the absence of the 817 bp insert with both tissue culture-derived and larvae-derived templates (data not shown). Gel purification and sequencing of these secondary products confirmed that they consisted of the *fp25k* and *lef-9* 5′ ends and the intergenic space between the two ORFs, but did not contain the IS. These results indicated that tissue culture- and larvae-derived PlxyMNPV-CL3 preparations contained genotypes in which the 817 bp insert sequence was either absent or present. A genotype missing the 817 bp insert was not detected in the final assembled contig of the genome, as the eight shotgun clones originating from this region all contained some or all of the 817 bp insert.

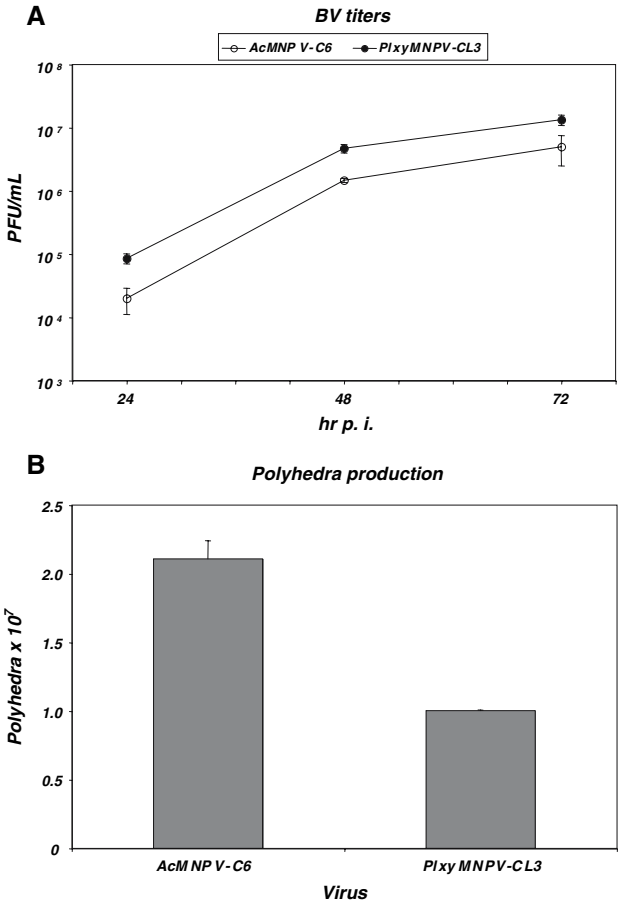

Fig. 5 **(A)** Budded virus produced by Sf9 cells infected with AcMNPV-C6 (○) and PlxyMNPV-CL3 (●), displayed as average plaque-forming units (pfu)/ml of three replicate samples/time point. **(B)** Polyhedra produced by Sf9 cells infected with AcMNPV-C6 and PlxyMNPV-CL3. Average polyhedra from three replicate infections/virus are shown. For both **(A)** and **(B)**, error bars represent one SD

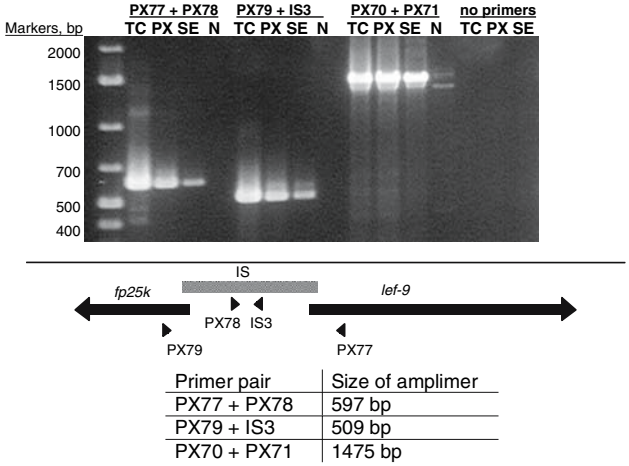

Fig. 6 PCR detection of the 817 bp IS in preparations of PlxyMNPV-CL3 DNA. Templates consisted of PlxyMNPV DNA from BV produced in tissue culture (TC), and from occluded virus (OV) harvested from *P. xylostella* (PX) and *S. exigua* (SE). For each primer pair, control reactions with no template (N) were run. The orientations and approximate positions of primers with respect to the IS are indicated by arrowheads. Control primers PX70 and PX71 anneal to a different region of the PlxyMNPV genome. The predicted sizes of amplimers generated by each primer pair are shown, as are the sizes of molecular weight markers

Discussion

Baculovirus genomes have clearly evolved by gene acquisition and loss [71]. Recombination between baculoviruses may also shape baculovirus genome evolution. An analysis by Jehle [72] found that AcMNPV likely acquired a portion of its polyhedrin gene by recombination with another NPV. The sequence of the PlxyMNPV-CL3 genome contains a striking instance of allelic replacement of a currently existing gene - *ie-2* - with a homologue from another divergent virus.

The AcMNPV *ie-2* gene stimulates optimal levels of baculovirus late promoter activation and *hr*-mediated plasmid DNA replication or stability in transient assays carried out in *S. frugiperda* Sf21 cells, but not in *T. ni* TN368 cells [73]. In addition, BmNPV *ie-2* was unable to substitute for AcMNPV *ie-2* in transient expression assays [74]. These results point to the prospect that the highly divergent *ie-2* gene carried by PlxyMNPV-CL3 may account for the differences in activity of PlxyMNPV and AcMNPV against *P. xylostella* larvae. However, AcMNPV mutants with deletions in the *ie-2* ORF killed *S. frugiperda* larvae with LD_{50} values equivalent to wild-type AcMNPV [75]. This result suggests, in contrast to the results of transient assays, that *ie-2* is not required for optimal replication in *S. frugiperda*. The role of *ie-2* in the virulence of PlxyMNPV-CL3 towards *P. xylostella* remains to be determined experimentally.

The region adjacent to *hr3* also was found to be a point of divergence between PlxyMNPV-CL3 and AcMNPV-C6. In the PlxyMNPV-CL3 genome, this region is marked by a deletion of the AcMNPV *ac86* ORF. In addition, three PlxyMNPV ORFs in this region (*plxy84*, *plxy85*, and *plxy90*) exhibited a relatively low degree of sequence conservation with homologous ORFs in AcMNPV. Sequence divergence in this area may contribute to the differences in the virulence of AcMNPV and related viruses towards different host species.

Another noteworthy difference between PlxyMNPV-CL3 and AcMNPV-C6 is the presence of an 817 bp sequence located between *fp25k* and *lef-9*. The location of this insert and the increased BV titers and reduced polyhedra production by PlxyMNPV-CL3 (Fig. 6) suggest that this insert resulted in an FP mutant phenotype. The CL3 clone was obtained from virus in infected *P. xylostella* hemolymph that had been passed through a *P. xylostella*

cell line and subsequently plaque-purified on an *H. virescens* cell line [9], and the insert may have originated from cellular DNA from one of those cell lines. Kariuki and McIntosh (2000 [11]) reported that PlxyMNPV-CL3 produces approximately twice as much $TCID_{50}$/ml and half as much polyhedra/cell as AcMNPV during infection of Sf21 cells. However, these authors found that PlxyMNPV-CL3 polyhedra contain virions and are infectious towards larvae [9]. Both tissue culture-derived and polyhedra-derived genomes carry the 817 bp insert, and it is possible that tissue culture passage of PlyxMNPV-CL3 has increased the proportion of genomes carrying this insert. If the 817 bp insert is causing an FP phenotype, the increased BV production of a genotype carrying this insert may enable it to persist in NPV populations arising from oral infection. The increased quantity of BV produced during infection may offer a selective advantage, such as a more rapid infection and inactivation of host hemocytes that contribute to the melanotic encapsulation of infected tissues [76].

The comparative analysis of genomic sequences from closely related viruses could provide insight into how baculoviruses adapt to new host species and overcome the defenses of current host species. Analysis of the PlxyMNPV-CL3 sequence has revealed some striking differences with other group I NPV genomes. Besides gene insertion, deletion and truncation, the differences in promoter motifs between PlxyMNPV-CL3 and AcMNPV, as well as point mutations in unidentified virulence determinants, may also contribute to the enhanced virulence of PlxyMNPV to the diamondback moth. This study will serve to guide future efforts to ascertain the molecular basis of differences in species-specific virulence among these viruses.

Acknowledgements The authors wish to thank Tad Sonstegard (USDA-ARS, Bovine Functional Genomics Laboratory) for the use of his GeneMachines Hydrohear, Wendy Sparks and Bryony Bonning (Iowa State University) for the gift of many oligonucleotides, Robert Farrar (USDA-ARS, Insect Biocontrol Laboratory) for larvae-derived polyhedra stocks of PlxyMNPV-CL3, Ellen Buckley (USDA-ARS, Insect Biocontrol Laboratory) for assistance with sequencing, and Stephen Rehner (USDA-ARS, Insect Biocontrol Laboratory) for helpful advice and discussion throughout the course of this study. Mention of trade names or commercial products in this publication is solely for the purpose of providing specific information and does not imply recommendation or endorsement by the U.S. Department of Agriculture.

References

1. B.C. Bonning. in *Comprehensive Molecular Insect Science*, eds. by L. Gilbert, K. Iatrou, S.S. Gill (Elsevier, Amsterdam; Boston, 2005), pp. 233–269
2. D.A. Theilmann, G.W. Blissard, B. Bonning, J.A. Jehle, R. O'Reilly D, G.F. Rohrmann, S. Thiem, J.M. Vlak. in Fauquet C.X., Mayo M.A., Maniloff J., Desselberger U., Ball L.A. (eds.), *Virus Taxonomy-Classfication and Nomenclature of Viruses 8th Report of the International Committee on the Taxonomy of Viruses* (Elsevier, Amsterdam, 2005), pp. 177–185
3. X. Huang, T.R. Davis, P. Hughes, A. Wood, J. Invertebr. Pathol. **69**, 234–245 (1997)
4. R. Armenta, A.M. Martinez, J.W. Chapman, R. Magallanes, D. Goulson, P. Caballero, R.D. Cave, J. Cisneros, J. Valle, V. Castillejos, D.I. Penagos, L.F. Garcia, T. Williams, J. Econ. Entomol. **96**, 649–661 (2003)
5. F.R. Hunter-Fujita, P.F. Entwhistle, H.F. Evans, N.E. Crook. *Insect Viruses and Pest Management* (Wiley, New York, 1998), pp. 7–26
6. M. Sarfraz, A.B. Keddie, L.M. Dosdall, Biocontrol Sci. Technol. **15**, 763–789 (2005)
7. H.A. Kadir, Potential of several baculoviruses for the control of diamondback moth and *Crocidolomia binotalis* on cabbages, in *Diamondback Moth and Other Crucifer Pests: Proceedings of the Second International Workshop*, ed. by N.S. Talekar (Asian Vegetable Research and Development Center, Tainan, Taiwan, 1992), pp. 185–192
8. R.R. Farrar, R.L. Ridgway, J. Agric. Urban Entomol. **16**, 187–196 (1999)
9. C.W. Kariuki, A.H. McIntosh, J. Econ. Entomol. **92**, 1093–1098 (1999)
10. R.R. Farrar, M. Shapiro, A.H. McIntosh, J. Entomol. Sci. **39**, 30–45 (2004)
11. C.W. Kariuki, A.H. McIntosh, C.L. Goodman, In Vitro Cell Dev. Biol. Anim. **36**, 271–276 (2000)
12. R.D. Possee, Virus Res. **5**, 43–59 (1986)
13. M.D. Summers, G.E. Smith, Tx. Ag. Expt. Stn. Bull. No. 1555 (1987)
14. D.E. Lynn, M. Shapiro, J. Invertebr. Pathol. **72**, 276–280 (1998)
15. D.R. O'Reilly, L.K. Miller, V.A. Luckow, *Baculovirus Expression Vectors* (W.H. Freeman and Company, New York, 1992)
16. J.A. Jehle, M. Lange, H. Wang, Z. Hu, Y. Wang, R. Hauschild, Virology **346**, 180–193 (2006)
17. M.D. Ayres, S.C. Howard, J. Kuzio, M. Lopez-Ferber, R.D. Possee, Virology **202**, 586–605 (1994)
18. S. Gomi, K. Majima, S. Maeda, J. Gen. Virol. **80**, 1323–1337 (1999)
19. O. Hyink, R.A. Dellow, M.J. Olsen, K.M. Caradoc-Davies, K. Drake, E.A. Herniou, J.S. Cory, D.R. O'Reilly, V.K. Ward, J. Gen. Virol. **83**, 957–971 (2002)
20. C.H. Ahrens, R.L. Russell, C.J. Funk, J.T. Evans, S.H. Harwood, G.F. Rohrmann, Virology **229**, 381–399 (1997)
21. R.L. Harrison, B.C. Bonning, J. Gen. Virol. **84**, 1827–1842 (2003)
22. J.G. de Jong, H.A. Lauzon, C. Dominy, A. Poloumienko, E.B. Carstens, B.M. Arif, P.J. Krell, J. Gen. Virol. **86**, 929–943 (2005)
23. H.A. Lauzon, P.B. Jamieson, P.J. Krell, B.M. Arif, J. Gen. Virol. **86**, 945–961 (2005)
24. J.D. Thompson, D.G. Higgins, T.J. Gibson, Nucleic Acids Res. **22**, 4673–4680 (1994)
25. S. Kumar, K. Tamura, M. Nei, Brief. Bioinform. **5**, 150–163 (2004)
26. P. Vail, G. Sutter, D. Jay, D. Gough, J. Invertebr. Pathol. **17**, 383–388 (1971)
27. R.D. Possee, G.F. Rohrmann. in *The Baculoviruses*, ed. by L.K. Miller (Plenum, New York, 1997), pp. 109–140
28. X. Chen, W.J. Zhang, J. Wong, G. Chun, A. Lu, B.F. McCutchen, J.K. Presnail, R. Herrmann, M. Dolan, S. Tingey, Z.H. Hu, J.M. Vlak, J. Gen. Virol. **83**, 673–684 (2002)
29. L. Li, Q. Li, L.G. Willis, M. Erlandson, D.A. Theilmann, C. Donly, J. Gen. Virol. **86**, 91–105 (2005)
30. C.X. Zhang, X.C. Ma, Z.J. Guo, Virology **333**, 190–199 (2005)
31. A.N. Volkoff, J. Rocher, P. Cerutti, M.C. Ohresser, Y. d'Aubenton-Carafa, G. Devauchelle, M. Duonor-Cerutti, J. Gen. Virol. **82**, 963–969 (2001)

32. T. Yanase, Y. Hashimoto, T. Kawarabata, Virus Genes **21**, 167–177 (2000)
33. D.K. Bideshi, S. Renault, K. Stasiak, B.A. Federici, Y. Bigot, J. Gen. Virol. **84**, 2531–2544 (2003)
34. E.A. Zemskov, W. Kang, S. Maeda, J. Virol. **74**, 6784–6789 (2000)
35. W. Kang, M. Suzuki, E. Zemskov, K. Okano, S. Maeda, J. Virol. **73**, 10339–10345 (1999)
36. A. Martins, S. Shuman, J. Biol. Chem. **279**, 18220–18231 (2004)
37. D. Durantel, L. Croizier, M.D. Ayres, G. Croizier, R.D. Possee, M. Lopez-Ferber, J. Gen. Virol. **79**, 629–637 (1998)
38. H. Beniya, S.C. Braunagel, M.D. Summers, Virology **240**, 64–75 (1998)
39. S.C. Braunagel, S.T. Williamson, S. Saksena, Z. Zhong, W.K. Russell, D.H. Russell, M.D. Summers, Proc. Natl Acad. Sci. USA **101**, 8372–8377 (2004)
40. S. Saksena, Y. Shao, S.C. Braunagel, M.D. Summers, A.E. Johnson, Proc. Natl Acad. Sci. USA **101**, 12537–12542 (2004)
41. S. Saksena, M.D. Summers, J.K. Burks, A.E. Johnson, S.C. Braunagel, Nat. Struct. Mol. Biol. **13**, 500–508 (2006)
42. D.R. O'Reilly, A.L. Passarelli, I.F. Goldman, L.K. Miller, J. Gen. Virol. **71**, 1029–1037 (1990)
43. D.D. Carson, L.A. Guarino, M.D. Summers, Virology **162**, 444–451 (1988)
44. D.D. Carson, M.D. Summers, L.A. Guarino, Virology **182**, 279–286 (1991)
45. S. Yoo, L.A. Guarino, Virology **202**, 746–753 (1994)
46. A.L. Passarelli, L.K. Miller, J. Virol. **67**, 2149–2158 (1993)
47. M. Kool, C.H. Ahrens, R.W. Goldbach, G.F. Rohrmann, J.M. Vlak, Proc. Natl Acad. Sci. USA **91**, 11212–11216 (1994)
48. E.A. Prikhod'ko, L.K. Miller, J. Virol. **72**, 684–692 (1998)
49. D. Mainz, I. Quadt, D. Knebel-Morsdorf, J. Virol. **76**, 5198–5207 (2002)
50. N. Imai, S. Matsumoto, W. Kang, J. Gen. Virol. **86**, 637–644 (2005)
51. S. Yoo, L.A. Guarino, Virology **202**, 164–172 (1994)
52. N. Imai, N. Matsuda, K. Tanaka, A. Nakano, S. Matsumoto, W. Kang, J. Virol. **77**, 923–930 (2003)
53. N. Imai, W. Kang, K. Iwabuchi, K. Sato, S. Maeda, Acta Virol. **44**, 199–202 (2000)
54. E.B. Carstens, Virology **161**, 8–17 (1987)
55. L.C. Cary, M. Goebel, B.G. Corsaro, H.G. Wang, E. Rosen, M.J. Fraser, Virology **172**, 156–169 (1989)
56. H.H. Wang, M.J. Fraser, L.C. Cary, Gene **81**, 97–108 (1989)
57. B. Beames, M.D. Summers, Virology **174**, 354–363 (1990)
58. P.D. Friesen, M.S. Nissen, Mol. Cell. Biol. **10**, 3067–3077 (1990)
59. B. Beames, M.D. Summers, Virology **168**, 344–353 (1989)
60. R.L. Harrison, M.D. Summers, J. Gen. Virol. **76(Pt 6)**, 1451–1459 (1995)
61. D.S. Bischoff, J.M. Slavicek, J. Virol. **71**, 1097–1106 (1997)
62. S. Katsuma, Y. Noguchi, C.L. Zhou, M. Kobayashi, S. Maeda, J. Gen. Virol. **80(Pt 3)**, 783–791 (1999)
63. L.H. Lua, M.R. Pedrini, S. Reid, A. Robertson, D.E. Tribe, J. Gen. Virol. **83**, 945–955 (2002)
64. D. Wu, F. Deng, X. Sun, H. Wang, L. Yuan, J.M. Vlak, Z. Hu, J. Gen. Virol. **86**, 2439–2444 (2005)
65. W.F. Hink, E. Strauss, J. Invertebr. Pathol. **27**, 49–55 (1976)
66. K.N. Potter, P. Faulkner, E.A. MacKinnon, J. Virol. **18**, 1040–1050 (1976)
67. M.J. Fraser, W.F. Hink, Virology **117**, 366–378 (1982)
68. T. Cusack, W.J. McCarthy, J. Gen. Virol. **70**, 2963–2972 (1989)
69. J.M. Slavicek, J. Podgwaite, C. Lanner-Herrera, J. Invertebr. Pathol. **59**, 142–148 (1992)
70. J.C. Bull, H.C. Godfray, D.R. O'Reilly, Appl. Environ. Microbiol. **69**, 2052–2057 (2003)
71. E.A. Herniou, J.A. Olszewski, J.S. Cory, D.R. O'Reilly, Annu. Rev. Entomol. **48**, 211–234 (2003)
72. J.A. Jehle, Virus Genes **29**, 5–8 (2004)
73. A. Lu, L.K. Miller, J. Virol. **69**, 6265–6272 (1995)
74. M.F. Berretta, M. Deshpande, E.A. Crouch, A.L. Passarelli, Virology **348**, 175–189 (2006)
75. E.A. Prikhod'ko, A. Lu, J.A. Wilson, L.K. Miller, J. Virol. **73**, 2460–2468 (1999)
76. J.O. Washburn, B.A. Kirkpatrick, L.E. Volkman, Nature **383**, 767 (1996)